# Dyadic and $\sqrt{3}$– Subdivision for Uniform Powell–Sabin Splines

**Evelyne Vanraes, Joris Windmolders,**
**Adhemar Bultheel, Paul Dierckx**

*Department of Computer Science, KULeuven.*
evelyne.vanraes@kuleuven.ac.be[1]

## Abstract

We give the two different possibilities for subdivision of Powell–Sabin splines on uniform triangulations. In the first case, dyadic subdivision, a new vertex is introduced on each edge between two old vertices. In the second case, $\sqrt{3}$–subdivision, a new vertex is introduced in the center of each triangle of the triangulation. We give subdivision rules for both cases.

## 1 Introduction

Widespread nowadays in commercial CAGD packages is the B–spline representation for curves, and correspondingly the tensor product B–spline representation for surfaces. The latter is, however, essentially restricted to rectangular domains, and therefore is not well suited for designing surfaces with an arbitrary number of edges. Farins Bézier triangles [2] are a worthwile alternative to represent piecewise polynomials on polygonal domains, but imposing smoothness conditions between the patches requires a great number of nontrivial relations between the coefficients to be satisfied. Another approach is a B–spline representation for Powell–Sabin (PS)–splines by Shi *et al.* [7], but their construction method has some serious drawbacks from the numerical point of view.

Dierckx [1] presented a normalized B–spline basis for PS–splines, which guarantees global $C^1$ smoothness for any choice of the coefficients, and resolves the numerical problems mentioned before. The subdivision schemes presented here are based on this representation and its geometrical interpretation. We consider the particular case of PS–splines on uniform triangulations which has the advantage that a fixed form for the PS–triangles can be used [5]. Subdivision gives the user local control when making changes to a surface, and it is a common technique for the graphical display of a surface. Another application is the design of wavelets using the lifting scheme. The subdivision rules are then used as a prediction step [6].

## 2 Uniform Powell–Sabin Splines

Consider a uniform triangulation $\Delta$ of a connected subset $\Omega \subset \mathbb{R}^2$ with polygonal boundary $\delta\Omega$. This triangulation consists of a number of equilateral triangles $\rho_j, j = 1, \ldots, t$ having vertices $V_i, i = 1, \ldots, n$ with Cartesian coordinates $(x_i, y_i)$. Let $\Delta^*$ be a Powell–Sabin refinement [4] of $\Delta$, which divides each macro triangle $\rho_j$ into six smaller triangles with a common vertex $Z_j$. This refinement can easily be found by drawing, for each triangle $\rho_j$, the bisector of its vertices (Figure 1(a)). Each of the $6t$ triangles resulting from the PS–refinement now becomes the domain triangle of a quadratic Bézier polynomial.

Such a quadratic Bézier polynomial over a nondegenerate triangle $\mathcal{T}(T_1, T_2, T_3)$ in the plane is

[1] Corresponding author

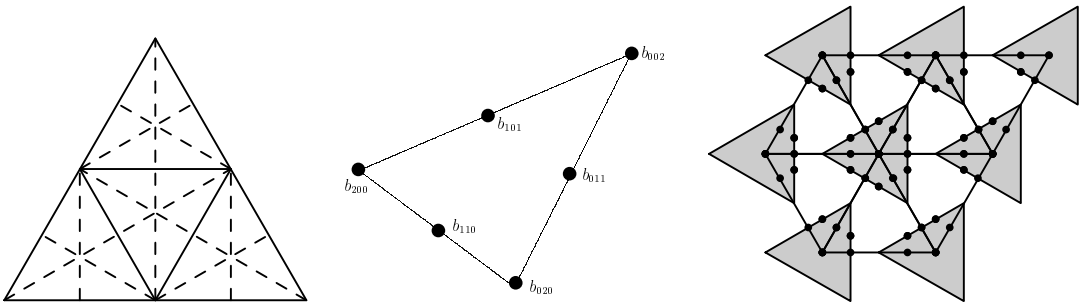


(a) (b) (c)

FIG. 1. (a) The dashed lines form a PS–refinement of the triangulation in solid lines. (b) Positions of the Bézier ordinates for a quadratic Bézier polynomial. (c) PS–points and a fixed form for the PS–triangles containing the PS–points.

defined by

$$b_{\mathcal{T}}(P) = b_{\mathcal{T}}(\tau) = \sum_{|\lambda|=2} b_\lambda B_\lambda(\tau), \tag{2.1}$$

in which $\lambda$ is the multi-index $\lambda = (\lambda_1, \lambda_2, \lambda_3)$, $|\lambda| = \lambda_1 + \lambda_2 + \lambda_3 = 2$, $\lambda_i \in \{0, 1, 2\}$ and $\tau = (\tau_1, \tau_2, \tau_3)$ are the barycentric coordinates with respect to $\mathcal{T}$ of a point $P$ in the plane : $P = \sum_{i=1}^{3} \tau_i T_i$ where $\sum_{i=1}^{3} \tau_i = 1$. The coefficients $b_\lambda$ are called Bézier ordinates, and

$$B_\lambda(\tau) = \frac{2!}{\lambda_1!\lambda_2!\lambda_3!} \tau_1^{\lambda_1} \tau_2^{\lambda_2} \tau_3^{\lambda_3} \tag{2.2}$$

are the Bernstein polynomials on the triangle.

The piecewise linear interpolant to the points $(\frac{\lambda}{2}, b_\lambda)$ is the Bézier net or control net, and is displayed schematically in Figure 1(b). The points $\frac{\lambda}{2}$, marked on the figure, are called Bézier domain ordinates. This representation has the convex hull property, pseudo–local control, is affine invariant, and is invariant under affine parameter transformations.

Now we consider the space of piecewise quadratic polynomials with $C^1$ continuity on $\Delta^*$, denoted by $S_2^1(\Delta^*)$. As already mentioned, each of the $6t$ triangles resulting from the PS–refinement becomes the domain triangle of a quadratic Bézier polynomial. Powell and Sabin [4] proved that the dimension of the space $S_2^1(\Delta^*)$ equals $3n$, so there exists a unique solution $S(x, y) \in S_2^1(\Delta^*)$ for the interpolation problem

$$S(V_k) = f_k, \quad \frac{\partial S}{\partial x}(V_k) = f_{x,k}, \quad \frac{\partial S}{\partial y}(V_k) = f_{y,k}, \quad k = 1, \ldots, n. \tag{2.3}$$

Thus given the function values and derivative values at each point $V_i$, the Bézier ordinates on the domain subtriangles are uniquely defined.

The PS–points of a vertex $V_i$ are those Bézier domain ordinates closest to $V_i$ on each edge of the PS–refinement $\Delta^*$ having $V_i$ as a vertex. $V_i$ itself is also a PS–point. The PS–triangle of the vertex $V_i$ is a triangle containing all the PS–points of $V_i$. An example of PS–points and PS–triangles is given in Figure 1(c).

Dierckx [1] showed that each piecewise polynomial $S(x,y) \in S_2^1(\Delta^*)$ has a unique normalized B–spline representation

$$S(x,y) = \sum_{i=1}^{n} \sum_{j=1}^{3} c_{i,j} B_i^j(x,y) \ , \quad (x,y) \in \Omega, \tag{2.4}$$

where the basis functions form a convex partition of unity and have local support: $B_i^j(x,y)$ is nonzero only on the so–called molecule $M_i$ of $V_i$, being the set of triangles $\rho_l$ that have $V_i$ as a vertex. The number of triangles in $M_i$ is called the molecule number $m_i$.

With each vertex $V_i$ three coefficients $c_{i,j}, i = 1, \ldots, n, \ j = 1,2,3$, the control points, are associated. One can prove that the control triangles, defined as $T_i(c_{i,1}, c_{i,2}, c_{i,3}), \ i = 1, \ldots, n$, are tangent to the surface at $S(V_i)$. These control triangles have the PS–triangles as their domain. We thus have a representation that shares the properties mentioned in the introduction of tensor product splines, but that is not restricted to rectangular domains. The advantage of using the split triangles in the PS–refinement as the domain for Bézier polynomials is that we have global $C^1$ continuity regardless of the choice of $c_{i,j}$: the continuity conditions between the Bézier triangles are automaticly satisfied. Dierckx also provides an algorithm to calculate the Bernstein–Bézier representation of the surface in an efficient and numerically stable way.

## 3 Subdivision

The goal of subdivision is essentially to calculate the B–spline representation (2.4) of a PS–spline surface on a refinement $\Delta'$ of the given $\Delta$. We consider two schemes: a dyadic scheme and a $\sqrt{3}$–scheme.

In [5], it is shown that for uniform PS–splines a fixed form for the PS–triangles can be used instead of determining the PS–triangle locally for each vertex. In a uniform triangulation only a limited number of molecule configurations appear. For each possible configuration an optimal shape of the PS-triangle can be calculated. It also turns out that for all molecule numbers the solution for a molecule with molecule number six can be used.

### 3.1 Dyadic subdivision

A first possibility for the refinement $\Delta'$ is dyadic subdivision. A new vertex is inserted on every edge in the middle of two old vertices. New edges are added between the new vertices and the old triangles are now each replaced by four smaller triangles. This is shown in Figure 2(a).

Windmolders *et al.* [5] prove that the Bézier ordinates of a surface can be determined as simple convex barycentric combinations of the control points $c_{ij}$ and that the control points after refinement can be written as simple barycentric convex combinations of the ones before refinement.

The new control triangles along an edge $V_iV_j \in \Delta$ are calculated as illustrated in Figure 2(b) , for the bottom edge of a triangle $\rho(V_i, V_j, V_k) \in \Delta$:

$$\begin{cases} c_1 &= \frac{1}{2}(c_{i,2} + c_{i,3}) \\ c_2 &= \frac{1}{2}c_{j,1} + \frac{1}{4}(c_{i,2} + c_{j,2}) \\ c_3 &= \frac{1}{2}c_{j,1} + \frac{1}{4}(c_{i,3} + c_{j,3}). \end{cases} \tag{3.1}$$

Rescaling the original control triangles is accomplished by

$$\begin{cases} c'_{i,1} &= \frac{2}{3}c_{i,1} + \frac{1}{6}(c_{i,2} + c_{i,3}) \\ c'_{i,2} &= \frac{2}{3}c_{i,2} + \frac{1}{6}(c_{i,3} + c_{i,1}) \\ c'_{i,3} &= \frac{2}{3}c_{i,3} + \frac{1}{6}(c_{i,1} + c_{i,2}) \end{cases} \tag{3.2}$$

for the control triangle at $V_i$.

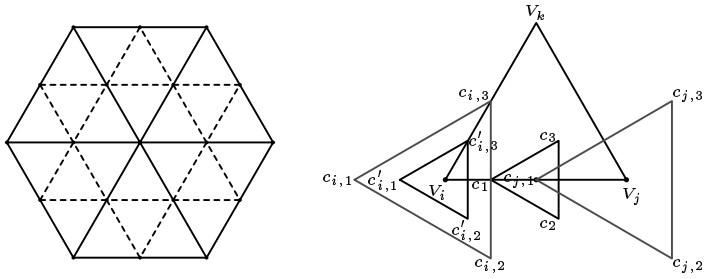


FIG. 2. (a) Principle of dyadic subdivision. (b) Detail for the bottom edge of a triangle $\rho(V_i, V_j, V_k) \in \Delta$.

A straightforward generalization of the dyadic split is the $n$-adic split where every edge is subdivided into $n$ segments and consequently every original face is split into $n^2$ subtriangles.

### 3.2 $\sqrt{3}$–subdivision

Recently we also developed a $\sqrt{3}$–scheme for the refinement $\Delta'$. $\sqrt{3}$–subdivision was first introduced by Kobbelt [3]. In this scheme we split every triangle in three new subtriangles by inserting a new vertex at the center of the old triangle. This introduces three new edges connecting the new vertex to the surrounding old vertices. We then rotate every original edge that connects two old vertices to connect the newly introduced vertices. Because the number of triangles increases in each step by a factor of 3 instead of 4, the $\sqrt{3}$–subdivision performs slower refinement than the dyadic split operation. Applying the $\sqrt{3}$–subdivision operator twice causes a uniform refinement with tri-section of every original edge and splitting of each original triangle into nine subtriangles: a tri-adic split. Hence one single refinement step can be considered as the square root of the tri-adic split. This is shown in Figure 3.

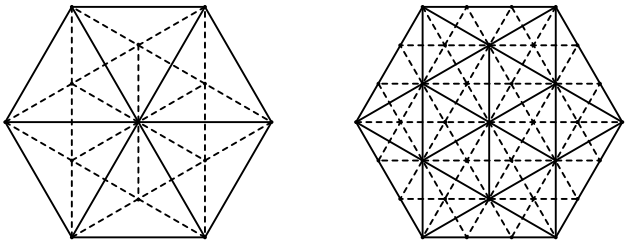

FIG. 3. Principle of $\sqrt{3}$–subdivision.

From the construction it follows that the lines of the PS–refinement, which are lines of $C^2$ discontinuity, coincide at successive levels of refinement. The PS–points of an old vertex have turned 30° counterclockwise around this vertex and the distance between the PS–points and the vertex is downscaled by a factor of 2. It is also clear that the old and new control triangles are coplanar. From these observations we can see that the new control points of the old vertices are given by

$$\begin{cases} c'_{i,1} &= \frac{2}{3}c_{i,1} + \frac{1}{3}c_{i,2} \\ c'_{i,2} &= \frac{2}{3}c_{i,2} + \frac{1}{3}c_{i,3} \\ c'_{i,3} &= \frac{2}{3}c_{i,3} + \frac{1}{3}c_{i,1} \end{cases} \tag{3.3}$$

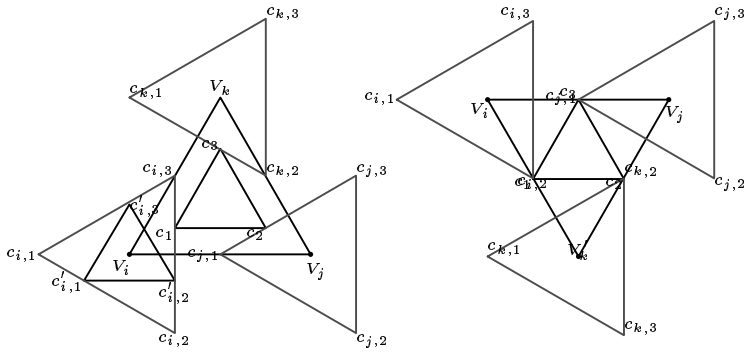


FIG. 4. (a)Detail of $\sqrt{3}$–subdivision for a triangle $\rho(V_i, V_j, V_k) \in \Delta$. (b) Detail for a triangle $\rho(V_i, V_j, V'_k) \in \Delta$ orientated in the other direction.

for the control triangle at $V_i$.

By means of Bézier subdivision we find the value of the Bézier ordinates in the control triangle of the new vertices in terms of the Bézier ordinates in the control triangles of the old vertices. As already mentioned, due to the fixed form of the PS–triangle, the Bézier ordinates can easily be written in terms of the control points and vice versa. This leads to the following formula for the control points according to a new vertex as shown in Figure 4(a)

$$\begin{cases} c_1 &= \frac{2}{3}c_{i,3} + \frac{1}{3}c_{i,2} \\ c_2 &= \frac{2}{3}c_{j,1} + \frac{1}{3}c_{j,3} \\ c_3 &= \frac{2}{3}c_{k,2} + \frac{1}{3}c_{k,1}. \end{cases} \tag{3.4}$$

For the case in which the old triangle in which we place the new vertex is oriented in the other direction (Figure 4(b)), we find analogously

$$\begin{cases} c_1 &= \frac{4}{9}c_{i,2} + \frac{2}{9}c_{i,3} - \frac{2}{9}c_{j,1} - \frac{1}{9}c_{j,2} + \frac{4}{9}c_{k',3} + \frac{2}{9}c_{k',1} \\ c_2 &= -\frac{2}{9}c_{i,2} - \frac{1}{9}c_{i,3} + \frac{4}{9}c_{j,1} + \frac{2}{9}c_{j,2} + \frac{4}{9}c_{k',3} + \frac{2}{9}c_{k',1} \\ c_3 &= \frac{4}{9}c_{i,2} + \frac{2}{9}c_{i,3} + \frac{4}{9}c_{j,1} + \frac{2}{9}c_{j,2} - \frac{2}{9}c_{k',3} - \frac{1}{9}c_{k',1}. \end{cases} \tag{3.5}$$

## 4 Discussion

The new basis functions corresponding to the control points after subdivision have smaller support and thus give the designer more local control when manipulating surfaces. Adjusting one control point only influences a small neighbourhood of the involved vertex. Furthermore, since the linear interpolant of the barycenters of the control triangles converges to the surface itself, subdivision is a common technique for displaying surfaces graphically.

The subdivision rules (3.1), (3.2), (3.3), (3.4) and (3.5) are also valid for uniform triangulations in which the triangles $\rho_j$ are not equilateral, but only all equal. The reasoning to come to the subdivision rules remains valid.

The $\sqrt{3}$–subdivision needs, in contrast to the dyadic scheme, special care at the boundaries. When rotating the old edges to connect the new vertices, we can only rotate the interior edges. Edge rotating at the boundaries is not possible since the opposite triangle is missing. As already

mentioned, the application of a second $\sqrt{3}$–step has the overall effect of a tri-adic split where each original triangle is replaced by nine new ones. In order to have this 1-to-9 split also for the boundary triangles we leave each boundary edge unchanged in the first step and add two new vertices on each boundary edge in the second step.

The $\sqrt{3}$–subdivision is in some sense slower then the dyadic refinement since the number of triangles increases by a factor of 3 instead of 4. This means we have a finer gradation of the hierarchy levels. If a prescribed target complexity must not be exceeded, we can have more levels of resolution.

A common technique to control the complexity of a refined surface is adaptive refinement. New vertices are inserted only in those regions of the surface where more detail is expected. Flat regions of the surface are well approximated by a few basis functions with large support. The $\sqrt{3}$–scheme is better suited to implement an adaptive refinement strategy without difficulties to join the triangles from different refinement levels in a consistent manner.

## Acknowledgement

This work is partially supported by the Belgian Program on Interuniversity Poles of Attraction, initiated by the Belgian State, Prime Minister's Office for Science, Technology and Culture, and by the Flemish Fund for Scientific Research (FWO Vlaanderen) project MISS (G.0211.02). The scientific responsibility rests with the authors.

## Bibliography

1. P. Dierckx. On calculating normalized Powell–Sabin B–splines. *CAGD*, 15(3):61–78, 1997.
2. G. Farin. Triangular Bernstein–Bézier patches. *CAGD*, 3(2):83–128, 1986.
3. Leif Kobbelt. $\sqrt{3}$-subdivision. In *Computer Graphics Proceedings*, Annual Conference Series. ACM SIGGRAPH, 2000.
4. M. J. D. Powell and M. A. Sabin. Piecewise quadratic approximations on triangles. *ACM Transactions on Mathematical Software*, 3:316–325, 1977.
5. J. Windmolders and P. Dierckx. Subdivision of Uniform Powell–Sabin splines. *CAGD*, 16:301–315, 1999.
6. J. Windmolders, E. Vanraes, P. Dierckx, and A. Bultheel. Uniform Powell–Sabin spline wavelets. TW Report 335, Department of Computer Science, Katholieke Universiteit Leuven, Belgium, February 2002.
7. W. Wang X. Shi, S. Wang and R. H. Wang. The $C^1$–quadratic spline space on triangulations. *Report 86004, Department of Mathematics, Jilin University, Changchun*, 1986.